Electron self-trapping in intermediate-valent SmB_6

S. Curnoe
Weizmann Institute of Science, Rehovot 76100, Israel

K. A. Kikoin*
Ben-Gurion University of the Negev, Beer-Sheva 84105, Israel

(Received 23 August 1999)

SmB_6 exhibits intermediate valence in the ground state and unusual behavior at low temperatures. The resistivity and the Hall effect cannot be explained either by conventional sf hybridization or by hopping transport in an impurity band. At least three different energy scales determine three temperature regimes of electron transport in this system. We consider the ground-state properties, the soft valence fluctuations, and the spectrum of band carriers in n-doped SmB_6. The behavior of excess conduction electrons in the presence of soft valence fluctuations, and the origin of the three energy scales in the spectrum of elementary excitations are discussed. The carriers which determine the low-temperature transport in this system are self-trapped electron-polaron complexes rather than simply electrons in an impurity band. The mechanism of electron trapping is the interaction with soft valence fluctuations.

I. INTRODUCTION

Samarium hexaboride is the first compound in which the phenomenon of intermediate valence (IV) has been seen directly by x-ray absorption,[1] but the theory which explains all properties of this compound within a unified physical model remains elusive in spite of unceasing efforts of theoreticians and experimentalists during the past 35 years. The conventional description of the electronic structure of SmB_6 in terms of a two-band promotion model results in a semiconductorlike spectrum with a gap Δ. This gap appears as a result of on-site hybridization between the narrow band formed by electrons from the samarium $4f$ shell and the wide conduction band formed by boron p states and samarium $5d$ states. The theory explains, at least phenomenologically, the main body of available experimental data.[2] However, the most intriguing properties of this material (as well as other IV semiconductors from the same family, i.e., SmS, TmSe, and YbB_{12}) cannot be described adequately within a framework of such a crude phenomenological picture. Among these properties are the very nature of the IV ground state, the origin of slow-valence fluctuations, and the low-temperature anomalies of various physical properties. Recent experimental studies of transport[3–5] and optical[6–8] properties revealed the existence of several energy scales in the low-energy excitation spectra and several temperature regimes in the low-temperature electron kinetics.

It is found that at least three different activation energies influence the behavior of electrons. The largest energy gap $\Delta_{opt} \approx 14-20$ meV is observed in the frequency-dependent conductivity and dielectric permittivity. Apparently, just this value should be ascribed to the hybridization gap Δ of the two-band model mentioned above. A substantially smaller value of $\Delta_{act} \approx 3-5$ meV is seen in the low-temperature resistivity and Hall effect measurements which display an activation-type temperature dependence in the interval $15 > T > 6$ K. This gap was also measured in tunneling experiments.[9] Below 6 K the resistivity is nearly temperature independent, and such behavior seems to be consistent with hopping transport in an impurity band separated by the gap Δ_{act} from the bottom of the conduction band. However, there is still no experimental consensus about the energy scales which control hopping. In Ref. 8 part of the low-T interval is presumed to be described by Mott's $T^{1/4}$ law for variable-range hopping with a scaling energy of $T_0 = 53$ K.[8] In another series of samples an activated term in the conductivity was observed with an activation temperature $T_a = 2.68$ K for $T < 3$ K,[3] although the derivation of an activation energy of the order of several K from measurements made in the same temperature interval does not look too trustworthy, in addition, the pressure dependence of the residual resistivity[4] is extremely strong, and it can hardly be fitted into a picture of noninteracting electrons in an impurity band. In any case, there is no room for additional excitation branches in the mean-field two-band theory, and adding extra localized states in the gap does not improve the situation. The standard hybridization model seems to be too simplistic, and we believe that the generic properties of the intermediate valence state can be described only within a framework that goes beyond the mean-field approximation.

In the present paper we offer a description of the low-energy spectrum of IV SmB_6 by treating the phenomenon of intermediate valence in rare-earth semiconductors in terms of an excitonic dielectric state. This approach was offered nearly two decades ago,[10] and its effectiveness was demonstrated later in explanation of anomalies in the vibration spectra of IV semiconductors.[11] Features of excitonic instability were seen also in studies of the dielectric-metal transition under pressure in the compounds $TmSe_{1-x}S_x$.[12] It is interesting that recently dramatic observations of a ferromagnetic phase in the n-doped divalent hexaborides CaB_6 and SrB_6 (Ref. 13) were interpreted in terms of conventional excitonic instability of Keldysh-Kopayev-Volkov-Rusinov type.[14]

The theory of intermediate-valence excitonic dielectric emphasizes the role of soft singlet excitonic states in the

formation of the ground IV state and valence fluctuations in the excitation spectrum. The IV state is described as a mixture of singlet $^7F_0$ states of divalent Sm(f^6) and the bound electron-hole pairs $f^5\tilde{b}$, where $\tilde{b}$ is the state of an electron promoted from the f shell to p orbitals spread over neighboring boron sites but having the same symmetry as the f electron in a central site. In some sense these states are electron-hole analogs of Zhang-Rice two-hole states known in the theory of low-energy states of CuO_2 planes in high-T_c perovskites.[15]

Here we consider the case of doped n-SmB_6 material. We study the behavior of excess conduction electrons in the presence of soft valence fluctuations, and discuss the origin of three energy scales seen in different temperature regimes. We show that the carriers which determine the low-temperature transport properties in this system are self-trapped electron-polaron complexes rather than simply electrons in an impurity band. The mechanism of electron trapping is the interaction with soft valence fluctuations.

II. GROUND STATE OF INTERMEDIATE-VALENCE SEMICONDUCTOR

SmB_6 together with ''golden'' SmS is considered to be a classical example of a non-magnetic IV semiconductor (see Ref. 2 and references therein). Both of these compounds possess a singlet ground state with intermediate valence $v \sim +2.6$. The main difference in the properties of these two compounds is that SmS transforms into an IV semiconductor only at finite pressure (or under the chemical pressure of rare-earth ions of smaller radius substituting for Sm) whereas SmB_6 possesses intermediate valence and concomitant anomalous properties at ambient pressure.

Apparently, differences in the electron band spectra of these two materials are the eventual source of differences in their properties. SmS at ambient pressure is known to be a normal semiconductor with a relatively wide gap in the energy spectrum $\Delta = 0.23$ eV. This gap divides the filled f levels of $Sm^{2+}(f^6)$ ions from the bottom of conduction band formed mainly by Sm d states. The $4f$ levels, in turn, form a nearly dispersionless valence band within a wide forbidden gap $E_g \gg \Delta$ between the conduction band and the conventional valence band formed mainly by p electrons of the chalcogen sublattice. At finite pressure the gap Δ is suppressed, but instead of collapsing to zero it transforms into a microgap Δ_μ at some critical pressure P_c, and the material acquires the properties of an IV semiconductor. On the other hand, the ''parent'' divalent hexaborides without a $4f$ shell (CaB_6, SrB_6), as well as trivalent LaB_6 with an empty $4f$ shell, have a band structure without a gap in the actual energy interval. The density of states near the Fermi level in hexaborides is predetermined by a single degenerate band with a minimum at the X point of the Brillouin zone. This band is formed mainly by p electrons of the boron sublattice with a small admixture of d states of the cation sublattice. It is nearly empty in divalent semimetallic hexaborides,[16,17] and more than half-filled in trivalent LaB_6.[18] Thus one can expect that the f level which is responsible for the intermediate valence of SmB_6 should cross this simple band. Indeed, conventional band calculations[19] give a band structure compatible with this presumption.

Despite the differences between the parent (unhybridized) spectra of SmS and SmB_6, the decisive similarity of these two cases is the closeness or overlapping of the highly correlated $4f$ levels of $Sm^{2+}(4f^6)$ and the degenerate conduction band. In SmB_6 these states overlap at ambient pressure, whereas in SmS the closeness is achieved under external pressure which induces the excitonic instability[10] at P_c. The closeness results in promotion of electrons to delocalized band states. Crucial is the fact that the number y of promoted electrons is the deviation from the divalent state in both $Sm^{(2+y)+}S$ and $Sm^{(2+y)+}B_6$ IV semiconductors. According to the conventional band scheme, which treats the ff interaction in a self-consistent mean-field approximation, the fp mixing results in the appearance of a hybridization gap Δ in the case of SmB_6 and a pseudogap in the IV phase of SmS. To take into account strong on-site correlations, this scheme should be modified.

The starting Hamiltonian for treating IV semiconductors is the Anderson lattice Hamiltonian supplemented by an interband Coulomb interaction (see, e.g., Ref. 20):

$$H = \sum_{\mathbf{k}\sigma} \epsilon_{\mathbf{k}} a^\dagger_{\mathbf{k}\sigma} a_{\mathbf{k}\sigma} + \sum_{\mathbf{m}} \sum_{\Lambda=0,\{\Gamma\mu\}} E_\Lambda |\mathbf{m}\Lambda\rangle\langle\mathbf{m}\Lambda| + \sum_{\mathbf{mk}\sigma\{\Gamma\mu\}} [V_{\mathbf{mk}\sigma,\Gamma\mu} a^\dagger_{\mathbf{k}\sigma} |\mathbf{m}\Gamma\mu\rangle\langle\mathbf{m}0| + \text{H.c.}] + \sum_{\mathbf{jkk}'\boldsymbol{\sigma}} U_{\mathbf{mkk}'} n_{\mathbf{m}f} a^\dagger_{\mathbf{k}\sigma} a_{\mathbf{k}'\sigma}. \quad (1)$$

Here $\epsilon_{\mathbf{k}}$ is a simple spin-degenerate dispersion law for the band electrons (we assume for the sake of simplicity that these electrons come from the boron $2p$ shells). The states $|\mathbf{m}\Lambda\rangle$ of the Sm ion at site $\mathbf{m}$ are represented by two configurations, $|\mathbf{m}\Lambda\rangle = |\mathbf{m}0\rangle \equiv |\mathbf{m}^7F_0\rangle$ for the divalent state $4f^6$ and $|\mathbf{m}\Lambda\rangle = |\mathbf{m}\Gamma\mu\rangle$ for the trivalent state $4f^5$. Γ stands for the multiplet $^6H_{5/2}$ of the $4f^5$ configuration which splits into a $\Gamma_7\mu$ doublet and a $\Gamma_8\mu$ quartet by the cubic crystal field Δ_{CF}; μ enumerates the states of corresponding irreducible representations, and $n_{\mathbf{m}f} = \Sigma_\mu |\mathbf{m}\Gamma\mu\rangle\langle\mathbf{m}\Gamma\mu|$ is the f-electron occupation number. The hybridization interaction describes the promotion of electrons from the f shell to the conduction band accompanied by a change of atomic configuration. The strong interband Coulomb interaction is given by $U_{\mathbf{mkk}'}$. The hybridization matrix element is $V_{\mathbf{mk}\sigma,\Gamma\mu} = \langle \mathbf{k}\sigma, \mathbf{m}\Gamma\mu | H | \mathbf{m}0\rangle$. At $T \ll \Delta_{CF}$ only the lowest doublet state Γ_7 should be taken into account, so one should deal with hybridization of two doubly degenerate states.

The strong intrashell interaction is inserted in the configuration change operators $X^{\Lambda\Lambda'}_{\mathbf{m}} = |\mathbf{m}\Lambda\rangle\langle\mathbf{m}\Lambda'|$. To make the hybridization problem solvable the nondiagonal operators are usually represented in a factorized form $X^{\Gamma 0}_{\mathbf{m}} = f_{\mathbf{m}\mu} b^\dagger_{\mathbf{m}}$ (see, e.g., Ref. 21), where $f_{\mathbf{m}\mu}$ and $b^\dagger_{\mathbf{m}}$ describe auxiliary fermion and boson fields which correspond to charge and spin degrees of freedom. This procedure gives reasonable results in the case of nearly integer valence, but in the IV state the spin charge separation procedure can hardly be useful even as a starting approximation. We prefer to use another approach[22] which seems to be adequate in the nonme-

tallic case when one can hope that hybridization will result in the separation of strongly correlated and weakly correlated bands in the energy space.

According to the prescription of this approach, we pick out the one-electron band Hamiltonian H_b which describes the hybridization of band electrons with the mean-field level ε_f, which is defined as the energy difference

$$\varepsilon_f = E_0 - E_{\Gamma_7},$$

where E_{Γ_7} is the lowest (doubly degenerate) state in the multiplet $f^5(^6H_{5/2})$, and then represent the Hamiltonian (1) in the form $H = H_b + \Delta H$. The term ΔH describes the excitations above the ground state. Then the mean-field spectrum in the actual energy interval can be described approximately by a Hamiltonian

$$H_b = \sum_{s=1,2} \sum_{\mathbf{k}\sigma} \varepsilon_s(\mathbf{k}) c^{\dagger}_{s,\mathbf{k}\sigma} c_{s,\mathbf{k}\sigma}. \tag{2}$$

Here

$$\varepsilon_{1,2}(\mathbf{k}) = \frac{1}{2}(\epsilon_{\mathbf{k}} + \varepsilon_f) \mp \sqrt{\frac{1}{4}(\epsilon_{\mathbf{k}} - \varepsilon_f)^2 + |V(\mathbf{k})|^2}, \tag{3}$$

where $e^{i\mathbf{m}\cdot\mathbf{k}} V(\mathbf{k}) = V_{\mathbf{mk}}$ from Eq. (1). Hybridization between p and f states due to the matrix elements $V(\mathbf{k})$ results in the wave functions

$$\begin{aligned} c_{1,\mathbf{k}\sigma} &= u_{\mathbf{k}} f_{\sigma} + v_{\mathbf{k}} c_{\mathbf{k}\sigma}, \\ c_{2,\mathbf{k}\sigma} &= -u_{\mathbf{k}\sigma} c_{\mathbf{k}\sigma} + v_{\mathbf{k}\sigma} f_{\sigma}, \end{aligned} \tag{4}$$

where the coefficients of the canonical transformation are

$$\begin{aligned} u_{\mathbf{k}} &= \frac{1}{2}\left[1 + \frac{\epsilon_{\mathbf{k}} - \varepsilon_f}{\sqrt{(\epsilon_{\mathbf{k}} - \varepsilon_f)^2 + 4|V(\mathbf{k})|^2}}\right], \\ v^2_{\mathbf{k}} &= 1 - u^2_{\mathbf{k}}. \end{aligned} \tag{5}$$

Since the band states and the f states have the same symmetry at the points X_7, R_7, Γ_7, and Δ_7,[20] a hybridization gap opens, and the lower band ε_1 is filled in the ground state of ''divalent'' SmB_6 because two electrons transferred from the f_{Γ_7} level to the (initially empty) band ε_1 fill it completely. Let us assume that the level ε_f crosses the band $\epsilon_{\mathbf{k}}$ in its lower part, so that the band $\varepsilon_1(\mathbf{k})$ has mainly f character. The square root in Eq. (3) can be expanded in $V(\mathbf{k})/[\varepsilon_{\mathbf{k}} - \varepsilon_f]$ for most of the Brillouin zone, and the Wannier states given by the operators $c_{1,\mathbf{m}\sigma} = N^{-1/2}\Sigma_{\mathbf{k}} \exp(i\mathbf{k}\cdot\mathbf{m}) c_{1,\mathbf{k}\sigma}$ can therefore be approximated by the following equations:

$$c_{1,\mathbf{m}\sigma} \approx f_{\mathbf{m}\sigma} + N^{-1/2} \sum_{\mathbf{k}} \sum_{\langle \mathbf{j} \rangle_{NN}} \frac{V(\mathbf{m}-\mathbf{j}) \exp[i\mathbf{k}\cdot(\mathbf{m}-\mathbf{j})]}{\epsilon_{\mathbf{k}} - \varepsilon_f} a_{\mathbf{j}}. \tag{6}$$

Here $\langle \mathbf{j} \rangle_{NN}$ are the nearest neighbors (boron sites) of a Sm ion in a given crystal cell, and $V(\mathbf{m}-\mathbf{j})$ is the Fourier transform of $V(\mathbf{k})$. The width T of the lower band is determined by a hopping integral, which can be estimated as

$$T_{\mathbf{mn}} \approx N^{-1/2} \sum_{\mathbf{kj}} \frac{V(\mathbf{m}-\mathbf{j}) V^*(\mathbf{n}-\mathbf{j}) \exp[i\mathbf{k}\cdot(\mathbf{m}-\mathbf{n})]}{\epsilon_{\mathbf{k}} - \varepsilon_f} \tag{7}$$

(here $\mathbf{j}$ are the nearest neighbors of both $\mathbf{m}$ and $\mathbf{n}$).

To study the *real* carriers, one should go beyond the mean-field Hamiltonian, i.e., take into account the term ΔH which includes, in particular, the interaction between holes in the narrow band $\varepsilon_1(\mathbf{k})$ and the electron-hole interaction between carriers in different bands. The former contribution stems from a strong Coulomb interaction between electrons in the Sm f-shell $U = \langle f_{\mathbf{m}} f_{\mathbf{m}} | U | f_{\mathbf{m}} f_{\mathbf{m}} \rangle$. This Hubbard interaction is reduced due to slight delocalization of Wannier functions,

$$\tilde{U} = \langle c_{1,\mathbf{m}} c_{1,\mathbf{m}} | U | c_{1,\mathbf{m}} c_{1,\mathbf{m}} \rangle = r^4 U,$$

where $r = \int S(\epsilon) u(\epsilon) d\epsilon$ is the reduction (nephelauxetic) factor.[22] This factor depends on the density of states $S(\epsilon)$ in the unhybridized band $\epsilon_{\mathbf{k}}$ [see Eq. (1)], and the coefficient $u(\epsilon)$ is that which appears in Eq. (4) but written as a function of energy. In our case the condition $T \ll \tilde{U}$ is assumed to be valid, and this means that no more than a single hole per site can be created in this narrow ''Hubbard'' band.

The upper band $\varepsilon_2(\mathbf{k})$ is formed mainly of p electrons, with an admixture of an f component in the states close to the bottom of this band. If the bottom of the conduction band is close to the center of the Brillouin zone,[20] Bogolyubov's coefficients for the electron wave function described by the operator $c_{2,\mathbf{k}}$ [Eq. (4)] are given by

$$v^2_k \approx 1 - \frac{|V_0|^2}{(\varepsilon_f - \epsilon_{\mathbf{k}})^2}, \quad u_k \approx \frac{V_0}{\varepsilon_f - \epsilon_{\mathbf{k}}}. \tag{8}$$

The Wannier operators $c_{2,\mathbf{m}}$ have the same form as Eq. (6), except that the sign of the denominator in the second term is negative. The dispersion in this band can be approximated by the effective-mass law

$$\varepsilon_2(k) \approx \Delta_0 + \frac{\hbar^2 (k - k_b)^2}{2m^*_c}, \tag{9}$$

where Δ_0 is the gap in the two-band spectrum [Eq. (3)]. Here k_b is the wave vector corresponding to the bottom of the empty band, and the effective mass can be estimated as

$$m^*_c / m_0 \approx [(\varepsilon_f - \epsilon_{k_b}) / V(k_b)]^2 = 1/\xi_c. \tag{10}$$

The effective mass is noticeably heavier than the bare mass m_0 of the conduction electron [experimentally, $m^*_c \sim 100 m_0$ (Ref. 8)]. We suppose that the hybridization gap is seen as the largest gap Δ_{opt} in the experiments mentioned in Sec. I.

Now, taking the energy of the state with filled lower band as a reference point in our calculations of the excitation energy spectrum, we have the effective Hamiltonian

$$\tilde{H}=\sum_{\mathbf{mn},\sigma} t_{\mathbf{mn}}\tilde{c}^{\dagger}_{1,\mathbf{m}\sigma}\tilde{c}_{1,\mathbf{n}\sigma}+\frac{\tilde{U}}{2}\sum_{\mathbf{m}\sigma} n_{1,\mathbf{m}\sigma}n_{1,\mathbf{m}-\sigma}$$

$$+\sum_{\mathbf{k}\sigma}\varepsilon_2(k)c^{\dagger}_{2,\mathbf{k}\sigma}c_{2,\mathbf{k}\sigma}+H_{12}, \tag{11}$$

where $t_{\mathbf{mn}}=\Sigma_{\mathbf{k}}e^{i\mathbf{k}\cdot(\mathbf{m}-\mathbf{n})}\varepsilon_1(\mathbf{k})$ and $\varepsilon_{1,2}(\mathbf{k})$ are given by Eq. (3). The electron states in the hopping term for hole excitations are dressed in projection operators, $\tilde{c}_{1,\mathbf{m}\sigma}=c_{1,\mathbf{m}\sigma}n_{1,\mathbf{m}-\sigma}$. This projection inserts the kinematic restriction for the hole motion: the hole can be created at a given site only provided the electron with the opposite spin is still at the same site. Therefore, the holes are practically immobile. The last term H_{12} is responsible for the electron-hole interaction,

$$H_{12}=\sum_{\mathbf{k}_1\mathbf{k}_2\mathbf{k}_3\mathbf{k}_4}\sum_{\sigma\sigma'} W(\mathbf{k}_1,\mathbf{k}_2,\mathbf{k}_3,\mathbf{k}_4)c^{\dagger}_{1,\mathbf{k}_1\sigma}c_{1,\mathbf{k}_2\sigma}c^{\dagger}_{2,\mathbf{k}_3\sigma'}c_{2,\mathbf{k}_4\sigma'}, \tag{12}$$

where W is derived from the Coulomb interaction [the last term in the Hamiltonian (1)].

The two-band Hamiltonian $\tilde{H}$ contains hybridization built into the electron and hole states, and the average occupation numbers $\bar{n}_{1\mathbf{i}f}\equiv\bar{n}_f$ are formally less than one in the lower ''Hubbard'' band ε_1. However, it should be emphasized that this deviation from integer value ($\bar{n}_f=1$ corresponds to the Sm^{2+} state) is not the true IV state. The one-electron picture given by the mean-field Hamiltonian H_b [Eq. (2)] implies that interband transitions given by the operator

$$S_q=\sum_{\mathbf{k}} c^{\dagger}_{2,\mathbf{k}+\mathbf{q}\sigma}c_{1,\mathbf{k}\sigma}=N^{-1}\sum_{\mathbf{mj}} e^{-i\mathbf{q}\cdot\mathbf{m}}c^{\dagger}_{2,\mathbf{m}+\mathbf{j}\sigma}c_{1,\mathbf{m}\sigma} \tag{13}$$

form the fundamental branch of elementary excitations in this semiconductor. However, free electron-hole excitations alone cannot explain the unusual properties of IV SmB_6. We believe that in the IV state an extra branch of charge transfer excitations exists. These are valence fluctuations, and are responsible for the unusual low-energy electron spectra and the numerous anomalies of the physical properties of SmB_6. According to the scenario suggested in Refs. 10 and 23 and verified in Ref. 11, the true IV ground state arises as a result of admixture of singlet excitonic states to the ground state of the same symmetry, and this admixture is non-negligible when the binding energy of the exciton is comparable with the band gap, i.e. when the system is close to the excitonic instability. To realize this scenario, one should construct the singlet exciton for the specific case of SmB_6.

According to the theory of IV rare-earth semiconductors,[10,23] the singlet exciton is a bound state of a hole in the samarium f shell and an electron spread over the p states of the surrounding nearest-neighbor (NN) boron atoms with the same crystal point symmetry as an f electron in the central cell . This state is constructed from electron-hole pairs [Eq. (13)] by means of an envelope function $F_{\mathbf{q}}(\mathbf{m}-\mathbf{j})$. When $\mathbf{q}=0$, the exciton operator can be written as

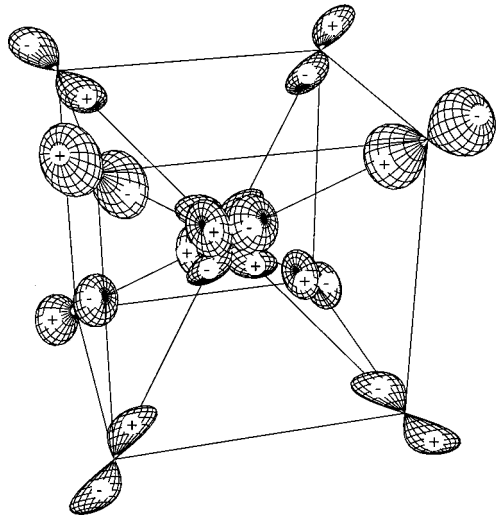

FIG. 1. A $4f$-orbital located at the center surrounded by eight p orbitals on the $(\frac{1}{2},\frac{1}{2},\frac{1}{2})$ corners. The signs of the p orbitals are chosen to have the same symmetry as the f orbital.

$$|\Psi_{ex}\rangle=N^{-1/2}\sum_{\mathbf{m}}\sum_{\langle\mathbf{j}\rangle_{NN}} F_0(\mathbf{m}-\mathbf{j})p^{\dagger}_{\mathbf{m}+\mathbf{j}\sigma}f_{\mathbf{m}\sigma}|0\rangle. \tag{14}$$

Here a basis of f and p orbitals is chosen. As mentioned above, the f electron has Γ_7 symmetry, and its angular dependence is determined by the xyz cubic harmonics. The envelope amplitude F_0 is a function of exciton energy E_{ex} (see, e.g., Ref. 10, where this function is calculated in the NN approximation). It also contains the phase factor which orders the phases of the p_x, p_y and p_z boron orbitals in accordance with the required symmetry (cf. Ref. 15),

$$F_0(\mathbf{m}-\mathbf{j})=F(E_{ex})(-1)^{M_{\mathbf{m},\mathbf{j}}}, \tag{15}$$

where the phase $(-1)^{M_{\mathbf{m},\mathbf{j}}}$ follows the arrangement shown in Fig. 1.

In fact, it will be shown below that the IV ground state resembles in some sense the Zhang-Rice (ZR) singlets,[15] which are believed to be formed in Cu-O planes of high-T_c materials. The Emery Hamiltonian,[24] which is the starting point for the description of hybridization between weakly interacting oxygen p electrons and strongly correlated copper d holes, is similar to the Anderson Hamiltonian describing the hybridization of nearly free b electrons in the conduction band with strongly localized electrons in samarium $4f$ shells. The difference is that the ZR bound states of a local Cu spin and a hole distributed over p orbitals of the surrounding O ions are formed as excitations in doped oxicuprates, while the IV singlets are formed in the ground state as bound states consisting of a hole in the f-shell of the Sm ion and an electron distributed over the p orbitals of the surrounding B ions of the cation sublattice. The binding mechanisms are the antiferromagnetic dp exchange in the ZR case and the Coulomb fp attraction in our case.

Now, inserting Eq. (15) into Eq. (14), we have

$$|\Psi_{ex}\rangle=F(E_{ex})N^{-1/2}\sum_{\mathbf{m}\sigma} P^{\dagger}_{\mathbf{m}\sigma}f_{\mathbf{m}\sigma}|0\rangle \tag{16}$$

where $P^{\dagger}_{\mathbf{m}\sigma}$ is a localized state which is defined as follows. SmB_6 has a simple cubic lattice structure, with an Sm atom in the center of each cell, and a B_6 group on each corner. To simplify the treatment, we approximate the electronic wave functions for the boron clusters by the p orbital directed along the diagonal of the cube (see Fig. 1). These orbitals are responsible for the covalent bonding between the boron clusters and Sm sublattice.[16] We introduce the linear combinations

$$p^{xyz}_{\mathbf{j}} \equiv \frac{1}{\sqrt{3}}[p_x(\mathbf{j})+p_y(\mathbf{j})+p_z(\mathbf{j})],$$

$$p^{\overline{xyz}}_{\mathbf{j}} \equiv \frac{1}{\sqrt{3}}[p_x(\mathbf{j})-p_y(\mathbf{j})+p_z(\mathbf{j})],$$

etc., which represent p-type electronic wave functions centred at $\mathbf{j}$ and oriented in the direction $\hat{x}+\hat{y}+\hat{z}$. In analogy with the Zhang-Rice construction, we write down a localized state for the Sm site $\mathbf{m}$ consisting of eight nearest-neighbor p orbitals oriented to have the same symmetry as a central f orbital, as shown in Fig. 1,

$$P_{\mathbf{m}\sigma}=\frac{1}{\sqrt{8}}[p^{xyz}_{\mathbf{m}+(1/2,1/2,1/2)}+p^{xyz}_{\mathbf{m}-(1/2,1/2,1/2)}+p^{\overline{xyz}}_{\mathbf{m}+(-1/2,1/2,1/2)} + p^{\overline{xyz}}_{\mathbf{m}-(-1/2,1/2,1/2)}+p^{x\overline{yz}}_{\mathbf{m}+(1/2,-1/2,1/2)}+p^{x\overline{yz}}_{\mathbf{m}-(1/2,-1/2,1/2)} + p^{xy\overline{z}}_{\mathbf{m}+(1/2,1/2,-1/2)}+p^{xy\overline{z}}_{\mathbf{m}-(1/2,1/2,-1/2)}]. \quad (17)$$

States on neighboring sites are nonorthogonal because of shared p electrons. Therefore, it is useful to make a canonical transformation to the orthonormalized Wannier or Bloch operators $d^{\dagger}$,

$$P^{\dagger}_{\mathbf{n}}=\sum_{\mathbf{m}} \lambda(\mathbf{m}-\mathbf{n})d^{\dagger}_{\mathbf{m}}=N^{-1/2}\sum_{\mathbf{k}} \beta^{1/2}_{\mathbf{k}}d^{\dagger}_{\mathbf{k}}e^{-i\mathbf{k}\cdot\mathbf{n}}, \quad (18)$$

where

$$\lambda(\mathbf{m}-\mathbf{n})=N^{-1}\sum_{\mathbf{k}} \beta^{1/2}_{\mathbf{k}}e^{i\mathbf{k}\cdot(\mathbf{m}-\mathbf{n})}, \quad (19)$$

$$\beta_{\mathbf{k}}=\frac{8}{3}\left[\cos^2\frac{k_x}{2}\sin^2\frac{k_y}{2}\sin^2\frac{k_z}{2}+\sin^2\frac{k_x}{2}\cos^2\frac{k_y}{2}\sin^2\frac{k_z}{2} + \sin^2\frac{k_x}{2}\sin^2\frac{k_y}{2}\cos^2\frac{k_z}{2}\right]. \quad (20)$$

Then the exciton operator acquires the form

$$|\Psi_{ex}\rangle=F(E_{ex})\frac{1}{N}\sum_{\mathbf{m}\sigma}\left[\lambda_0 d^{\dagger}_{\mathbf{m}\sigma}+\sum_i \lambda_i\sum_{\langle\mathbf{n}\rangle_i} d^{\dagger}_{\mathbf{n}\sigma}\right]f_{\mathbf{m}\sigma}|0\rangle \equiv \frac{1}{N}\sum_{\mathbf{m}} |\psi_{\mathbf{m}}\rangle. \quad (21)$$

TABLE I. The coefficients $\lambda(\mathbf{m}-\mathbf{n})$, where $\mathbf{m}-\mathbf{n}=i\hat{x}+j\hat{y}+k\hat{z}$.

	(i,j,k)	λ
λ_0	(0,0,0)	0.935
λ_1	(1,0,0)	−0.104
λ_2	(1,1,1)	0.056
λ_3	(1,1,0)	−0.052

Here the index $i=1,2\ldots$ enumerates the coordination spheres, and the coefficients λ_i fall rapidly with increasing distance (see Table I).

By construction, the states $|0\rangle$ and $|\Psi_{ex}\rangle$ belong to the set of eigenstates of the Hamiltonian $\tilde{H}$ [Eq. (11)], with nonlocal terms $\tilde{H}_{1h}=\Sigma_{\mathbf{m}\neq\mathbf{n},\sigma}t_{\mathbf{mn}}\tilde{c}^{\dagger}_{1,\mathbf{m}\sigma}\tilde{c}_{1,\mathbf{n}\sigma}$ and δH_{12} (defined below) excluded. However, these nonlocal interactions are responsible for forming the IV state. In a simplest approximation we restrict ourselves by considering only the first term $\sim\lambda_0$ in the expansion (21) and take the nonlocal interaction in the form

$$\delta H_{12}=\sum_{\mathbf{mn}\sigma} W(\mathbf{m}-\mathbf{n})f^{\dagger}_{\mathbf{m}\sigma}f_{\mathbf{n}\sigma}f^{\dagger}_{\mathbf{n}\sigma}d_{\mathbf{m}\sigma}+\text{H.c.} \quad (22)$$

This component of electrostatic interaction violates the point crystalline symmetry and induces fp hybridization at the site $\mathbf{m}$ in the presence of a hole in the neighboring cell $\mathbf{n}$. The operator δH_{12} has a property

$$\delta H_{12}|\psi_{\mathbf{m}}0_{\mathbf{n}}\rangle=W(\mathbf{m}-\mathbf{n})|0_{\mathbf{m}}0_{\mathbf{n}}\rangle,$$

where $0_{\mathbf{n}}$ stands for the cell $\mathbf{n}$ in the ground-state configuration. Thus this interaction intermixes the states $|0\rangle\equiv\Pi_{\mathbf{n}}|0_{\mathbf{n}}\rangle$ and $|\Psi_{ex}\rangle$. The mixing constant is $w=\langle 0|\delta H_{12}|\Psi_{ex}\rangle = zF(E_{ex})\lambda_0 W$, where z is the coordination number for the Sm sublattice and W is the NN interaction matrix element. After diagonalization the local neutral states in each cell $\mathbf{m}$ are represented by the linear combinations

$$|\overline{0}_{\mathbf{m}}\rangle=\cos\theta|0_{\mathbf{m}}\rangle+\sin\theta|\psi_{\mathbf{m}}\rangle,$$
$$|\overline{\psi}_{\mathbf{m}}\rangle=-\cos\theta|\psi_{\mathbf{m}}\rangle+\sin\theta|0_{\mathbf{m}}\rangle, \quad (23)$$

where $\tan 2\theta\approx 2w/E_{ex}$, and the valence is determined by the value of $\sin^2\theta$. As mentioned, the local states (23) are in some sense the electron-hole analogs of two-hole Zhang-Rice singlets and triplets.[15,25] Finally, the ground state of the IV semiconductor is

$$|\Psi^{(iv)}_0\rangle=\prod_{\mathbf{m}} |\overline{0}_{\mathbf{m}}\rangle, \quad (24)$$

and the low-lying local excitations are described by the vector

$$|\Psi^{(iv)}_{ex}\rangle=N^{-1}\sum_{\mathbf{m}} |\overline{\psi}_{\mathbf{m}}\rangle\langle\overline{0}_{\mathbf{m}}|\Psi^{(iv)}_0\rangle. \quad (25)$$

The valence and the energy scale of these local excitations (valence fluctuations) are characterized by the degree of admixture of the excitonic state, in which an electron is promoted to a loosely bound ''molecular orbit'' $P_{\mathbf{m}}$. If the exciton energy E_{ex} is small enough (the exciton binding energy is comparable with the gap width), the value of $\sin^2\theta$ is close to 1/2. Also keeping in mind the mean-field part of hybridization given by Eq. (4), we conclude that in this case the valence

$$n_v = 3 - \overline{n}_f + \sin^2\theta \tag{26}$$

can exceed 2.5 both in SmS and SmB_6. Thus the large deviation of the valence value from the integer value and the softness of local valence fluctuations are, apparently, the correlated phenomena. Further discussion of internal consistency of the model can be found in the last section.

III. TRAPPING OF CONDUCTION ELECTRONS AND HOPPING CONDUCTIVITY

The samples of good quality which were studied in the experiments of the past decade mentioned in Sec. I are *n*-type semiconductors at low temperature, unlike the *p*-type samples of the first generation.[26] The electron concentration in these samples is estimated at $n_e \sim 10^{17}$ cm^{-3} at ambient pressure and liquid helium temperature.[3,4] In order to interpret the transport properties of these samples one should determine the spectrum of electrons at the bottom of the conduction band in the presence of soft valence fluctuations. In our model the local valence fluctuations arise as transitions between the states $|\overline{0}_{\mathbf{m}}\rangle$ and $|\overline{\psi}_{\mathbf{m}}\rangle$ given by Eq. (23). It is known that these valence fluctuations are the source of strong anomalies in the vibration spectra because the characteristic time τ_{vf} of valence fluctuations is close to phonon times $\tau_{ph} \sim \omega_{ph}^{-1} \sim 10^{-13}$ s. Therefore, one can expect that these ''slow'' excitations could dress the carriers and form an electron-polaron cloud similar to the phonon cloud which results in polaron self-trapping in dielectric crystals (see, e.g., Ref. 27).

To describe electron self-trapping we start with a Hamiltonian including the interaction between the conduction electron and the *local* valence fluctuations in a single lattice site $\mathbf{n}=0$;

$$H_e = \sum_{\mathbf{k}} \varepsilon(\mathbf{k}) c_{\mathbf{k}}^{\dagger} c_{\mathbf{k}} + \Omega_0 A^{\dagger} A + \sum_{\mathbf{k}_1,\mathbf{k}_2} [W_{vf}(\mathbf{k}_1,\mathbf{k}_2) c_{\mathbf{k}_1}^{\dagger} c_{\mathbf{k}_2} A^{\dagger} + \text{H.c.}]. \tag{27}$$

This Hamiltonian stems from our basic Hamiltonian (11). It includes the electrons in the upper conduction band (the spin summation and band index $s=2$ are omitted). Only the term which corresponds to momentary, local redistributions of charge and valence at the site of the excitation due to the interaction with the charge carrier is retained in H_{12}. The valence fluctuations with the energy Ω_0 are described by the local operator $A^{\dagger} = |\overline{\psi}\rangle\langle\overline{0}|$. This excitation is in fact a charge transfer between the periphery and the center of the cell. The ''breathing'' mode Ω_0 describes the polarization of Sm ions in the cation sublattice that accompanies the propagation of an excess conduction electron (predominantly, over the samarium sublattice; see below).

The matrix element $W_{vf}(\mathbf{k}_1,\mathbf{k}_2)$ is given by the integral

$$W_{vf}(\mathbf{k}_1,\mathbf{k}_2) = \int d\mathbf{r}_1 d\mathbf{r}_2 \overline{\psi}_{ex}^{*}(\mathbf{r}_1)\overline{\psi}_0(\mathbf{r}_1) W(\mathbf{r}_1,\mathbf{r}_2)\psi_{\mathbf{k}_1}^{*}(\mathbf{r}_2)\psi_{\mathbf{k}_2}(\mathbf{r}_2)$$

where $\psi_{\mathbf{k}}(\mathbf{r})$ are the Bloch functions for the conduction electrons, and $\overline{\psi}_{ex}^{*}(\mathbf{r})$ and $\overline{\psi}_0(\mathbf{r})$ are the wavefunctions of the states created by the operators (23). Their product is

$$\overline{\psi}_{ex}^{*}(\mathbf{r})\overline{\psi}_0(\mathbf{r}) \equiv D(\mathbf{r}) = \frac{1}{2}\{\sin 2\theta[\rho_p(\mathbf{r}) - \rho_f(\mathbf{r})] - \cos 2\theta f_{xyz}(\mathbf{r}) d_{xyz}(\mathbf{r})\}, \tag{28}$$

where $\rho^f(\mathbf{r}) = |f_{xyz}(r)|^2$ is the *f*-electron density in the center of the cell (see Fig. 1), and $\rho^p(\mathbf{r}) = F^2(E_{ex})\lambda_0^2 |d_{xyz}(r)|^2$ is the *p*-electron density in a central cell given by the first term on the right-hand side of Eq. (21). The conduction-electron density operator $\rho_{\mathbf{k}_1,\mathbf{k}_2}(\mathbf{r}_1) = \psi_{\mathbf{k}_1}^{*}(\mathbf{r}_2)\psi_{\mathbf{k}_2}(\mathbf{r}_2)$ is determined by the Bloch functions (4). Near the bottom of conduction band this operator can be approximately presented as

$$\rho_{\mathbf{k}_1,\mathbf{k}_2}(\mathbf{r}_1) \approx \rho^f(\mathbf{r}) + \zeta_c \rho^p_{\mathbf{k}_1,\mathbf{k}_2}(\mathbf{r}_1) \tag{29}$$

by means of Eq. (8). Here

$$\zeta_c = V_0^2/\varepsilon_{fb}^2, \tag{30}$$

$$\rho^p_{\mathbf{k}_1,\mathbf{k}_2} = \sum_{\langle \mathbf{j}\rangle_{NN}} e^{-i(\mathbf{k}_1-\mathbf{k}_2)\cdot\mathbf{j}} |\psi_{\mathbf{j}}(\mathbf{r}_1)|^2, \tag{31}$$

and $\varepsilon_{fb} = \varepsilon_f - \varepsilon_{k_b}$. Then the coupling constant in the Hamiltonian (27) acquires the form

$$W_{vf}(\mathbf{k}_1,\mathbf{k}_2) \approx w_0 + w_1 \tilde{\beta}_{\mathbf{k}_1-\mathbf{k}_2}, \tag{32}$$

where

$$w_0 = \int d\mathbf{r}_1 d\mathbf{r}_2 D(\mathbf{r}_1) W(\mathbf{r}_1,\mathbf{r}_2)\rho^f(\mathbf{r}_2),$$

$$w_1\tilde{\beta}_{\mathbf{k}_1-\mathbf{k}_2} = \int d\mathbf{r}_1 d\mathbf{r}_2 D(\mathbf{r}_1) W(\mathbf{r}_1,\mathbf{r}_2)\rho^p_{\mathbf{k}_1,\mathbf{k}_2}(\mathbf{r}_2+\mathbf{j}).$$

The structure factor $\tilde{\beta}_{\mathbf{k}}$ is given by

$$\tilde{\beta}_{\mathbf{k}} = 8\cos\frac{k_x}{2}\cos\frac{k_y}{2}\cos\frac{k_z}{2}. \tag{33}$$

It is seen that the first term w_0 dominates in the electron-exciton interaction; therefore, we begin with a calculation of the electron self-energy induced by this term within the lowest order of perturbation theory. The theory which allows

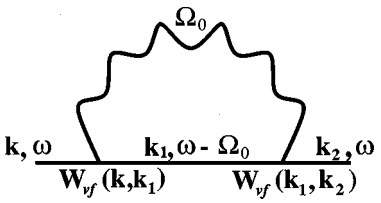

FIG. 2. The self-energy diagram corresponding to Eq. (37). The straight line represents a conduction electron, and the wavy line represents a soft valence fluctuation.

inclusion of nonlocal corrections due to small term $\sim w_1$ in Eq. (32) is described in the Appendix. We calculate the electron Green's function in the Matsubara representation,

$$G_{\mathbf{k}\mathbf{k}'}(\omega_n)=\int_0^\beta \langle T_\tau c_{\mathbf{k}}(\tau)c^\dagger_{\mathbf{k}'}\rangle e^{i\omega_n\tau}d\tau \tag{34}$$

$[\omega_n=(2n+1)\pi T]$, interacting with a localized valence fluctuation mode Ω_0 described by the propagator

$$D(\omega_m)=-\frac{2\Omega_0}{\omega_m^2+\Omega_0^2} \tag{35}$$

$[\omega_m=2\pi mT]$. The Dyson equation for the electron Green's function is

$$G_{\mathbf{k},\mathbf{k}'}(\omega_n)=G^0_{\mathbf{k}}(\omega)\left[\delta_{\mathbf{k},\mathbf{k}'}+\sum_{\mathbf{k}_2}\Sigma_{\mathbf{k},\mathbf{k}_2}(\omega_n)G_{\mathbf{k}_2,\mathbf{k}'}(\omega_n)\right]. \tag{36}$$

In the lowest order of perturbation theory the self-energy $\Sigma_{\mathbf{k}_1,\mathbf{k}'}(\omega_n)$, after carrying out an analytic continuation into the region of real frequencies, acquires the form (see Fig. 2)

$$\Sigma^R_{\mathbf{k},\mathbf{k}_2}(\omega)=\sum_{\mathbf{k}_1} W_{vf}(\mathbf{k},\mathbf{k}_1)W_{vf}(\mathbf{k}_1,\mathbf{k}_2)\mathcal{P}_{\mathbf{k}_1}(\omega,\Omega_0), \tag{37}$$

where

$$\mathcal{P}_{\mathbf{k}_1}(\omega,\Omega_0)=\int_{-\infty}^{\infty}\frac{d\epsilon}{2\pi}\frac{\mathrm{Im}\,D^R(\epsilon)}{\epsilon+\varepsilon(\mathbf{k}_1)-\omega-i\delta} \times\left(\tanh\frac{\varepsilon(\mathbf{k}_1)}{2T}+\coth\frac{\epsilon}{2T}\right). \tag{38}$$

Approximating the nonlocal potential $W_{vf}(\mathbf{k},\mathbf{k}_1)$ by its local part w_0, we come immediately to the following equation

$$1-w_0^2 m(\omega)m(\omega-\Omega_0)=0, \tag{39}$$

where $m(\omega)=\Sigma_{\mathbf{k}}G^0_{\mathbf{k}}(\omega)$.

In close analogy with the polaron self-trapping effect,[27] one can expect that the attractive polarization potential with an effective coupling constant

$$g^0(\omega)=w_0^2\sum_{\mathbf{k}_2} G^0_{\mathbf{k}_2}(\omega-\Omega_0)$$

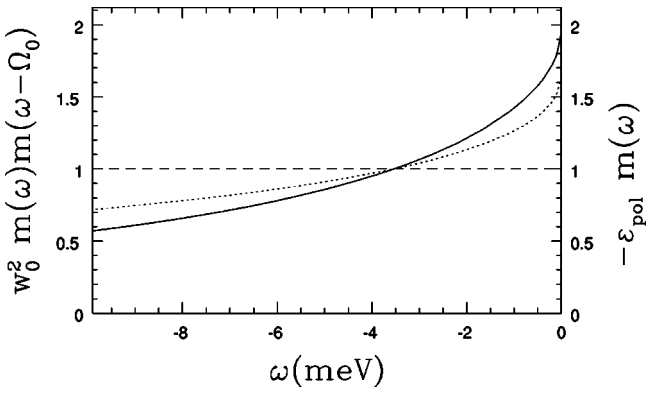

FIG. 3. Graphical solutions to Eqs. (39) (solid line) and (43) (dotted line) using $\epsilon_0=5$ meV, $m^*=100m_0$, $\Omega_0=5.5$ meV, $w_0=25$ meV, and $\varepsilon_{pol}=21$ meV.

results in the appearance of bound electron-polaron states. As usual in three-dimensional problems, the threshold value of the attractive potential determines the onset of the bound state. To find the constraints on the solutions with negative energy (corresponding to bound states), we examine the function $m(\omega)$ defined in Eq. (39):

$$m(\omega)=\int_{-\pi}^{\pi}\frac{dk_x dk_y dk_z}{(2\pi)^3}\frac{1}{\omega-\epsilon(\mathbf{k})}. \tag{40}$$

At $\omega=0$ the integral may be evaluated numerically (see the Appendix). Figure 3 demonstrates the graphical solution of Eq. (39) for a reasonable set of model parameters. The value of $\Omega_0=5.5$ meV correlates the experimentally observed peak in optical reflectivity spectra,[6,7] and the binding energy of localized $\omega_1\approx 3.5$ meV is in good agreement with the activation energy registered in multiple optical and transport measurements in the temperature interval 6–14 K (see Ref. 5 and references therein).

We have demonstrated the existence of a self-trapped state in the simplest approximation, whereby the local polarization mode is taken into account in second-order perturbation theory. However, the values of the parameters necessary to achieve reasonable agreement with experiment give for the dimensionless coupling constant $\alpha=w_0/\Omega_0$ the value of $\alpha\approx 4.5$. This means that in fact we are in a strong-coupling limit, and a more refined treatment is necessary. The generalization of the theory to the strong-coupling limit can be done in close analogy with the theory of small polaron. One can make the canonical transformation $\tilde{c}_{\mathbf{k}}=e^{-S}c_{\mathbf{k}}e^{S}$, where

$$S=\sum_{\mathbf{kq}}\frac{W_{vf}(\mathbf{k},\mathbf{q})}{\Omega_0}(c^\dagger_{\mathbf{k}}c_{\mathbf{k}+\mathbf{q}}A^\dagger_{\mathbf{q}}-c^\dagger_{\mathbf{k}+\mathbf{q}}c_{\mathbf{k}}A_{-\mathbf{q}}) \tag{41}$$

(see, e.g., Ref. 28). We have seen above that the local term w_0 is dominant in electron-exciton coupling constant [Eq. (32)]. Then neglecting the contribution of the ''tail'' w_1 we come to purely local interaction at a given site $\mathbf{m}=\mathbf{0}$, namely, $\delta H_{12}=w_0c^\dagger_{\mathbf{0}}c_{\mathbf{0}}(A^\dagger_{\mathbf{0}}+A_{\mathbf{0}})$. Eliminating this interaction by means of a canonical transformation [Eq. (41)], one comes to the effective Hamiltonian

$$\tilde{H}_e = e^{-S} H_e e^{S} = \sum_{\mathbf{m}} \varepsilon_f c^{\dagger}_{\mathbf{m}} c_{\mathbf{m}} + \sum_{\mathbf{m},\mathbf{n}\neq\mathbf{0}} T_{\mathbf{mn}} c^{\dagger}_{\mathbf{m}} c_{\mathbf{n}} + \Omega_0 A^{\dagger}_{\mathbf{0}} A_{\mathbf{0}} - \varepsilon_{pol} c^{\dagger}_{\mathbf{0}} c_{\mathbf{0}} - \sum_{\mathbf{m}\neq\mathbf{0}} (T_{\mathbf{m0}} c^{\dagger}_{\mathbf{0}} c_{\mathbf{m}} e^{-\alpha(A^{\dagger}_{\mathbf{0}} - A_{\mathbf{0}})} + \text{H.c.}). \quad (42)$$

Now the main part of electron-exciton interaction is taken into account exactly, and it is contained in the polaron shift. This shift induces the local scattering at the site **0** which is given by the operator $\varepsilon_{pol} \Sigma_{\mathbf{k}_1,\mathbf{k}_2} c^{\dagger}_{\mathbf{k}_1} c_{\mathbf{k}_2}$, where $\varepsilon_{pol} = \alpha w_0$. The local scattering can be inserted in the self-energy of the conduction electron in the same manner as it was done in second order of perturbation theory in Eq. (36). However, now the calculation is exact, and instead of Eq. (39) one has

$$0 = 1 + \varepsilon_{pol} \sum_{\mathbf{k}} [\omega - \varepsilon(\mathbf{k})]^{-1} = 1 + \varepsilon_{pol} m(\omega), \quad (43)$$

which can be solved by using the same approximation as in Eq. (39). In any case the electron can be trapped by local valence fluctuations provided the polaron shift $\varepsilon_{pol} = \alpha w_0$ given by the bound solution of Eq. (39) exceeds the characteristic kinetic energy of the electrons near the bottom of the conduction band. Therefore the effective mass enhancement due to pf hybridization favours the formation of a self-trapped state.

In Fig. 3 we show a bound state solution with energy 3.5 meV in agreement with the activation energy observed in transport measurements and absorption edges in optical experiments. In both cases the coupling constant w_0 is treated as a free parameter. In the second-order perturbation calculation w_0 is determined to be 25 meV, which, as we have discussed above, indicates that our solution lies in the limit of strong coupling. In the non-perturbative calculation we find that $\varepsilon_{pol} = w_0^2/\Omega_0 = 21$ meV, which implies that $w_0 = 11$ meV. Because we are in the strong-coupling limit we do expect a deviation between the exact calculation and the second-order perturbation result. However, our results are close enough to suggest that the physical content of the perturbative calculation is correct, that is, that an electron may bind to a single local valence fluctuation and the result is a localized electron-valence fluctuation complex. Moreover, we also observe that our results are not particularly sensitive to the input parameters, and are therefore not the result of any special ''fine tuning.'' All of this is a consequence of the fact that the relevant energies are all roughly the same: $\Omega_0 = 5.5$ meV, $\hbar^2/a^2 m^* = 5$ meV and $\Delta_{act} = 3.5$ meV.

The last term in the effective Hamiltonian (42) is responsible for the exciton-assisted hopping in an electron-polaron band. The electron self-trapping can occur around any arbitrary lattice site, so the trapped particle can move from a given cell to the neighboring cells by a mechanism which resembles polaron propagation.[27,28] Therefore, the electron-polaron drift in an electric field is responsible for the conductivity at $T \to 0$ in n-type SmB_6. We leave a systematic treatment of electron transport in IV semiconductors for future publications, and conclude this article by qualitative discussion of anomalous low-T behavior of SmB_6 mentioned in Sec. I.

IV. CONCLUDING REMARKS

As a result of the above analysis, one can understand the mechanism of reduction from the eV energy scale characteristic of initial Hamiltonian (1) down to meV scale of low-lying charge excitations in the n-type material. First, at the mean-field level of approximation [Eqs. (2)–(10)] the gap $\Delta_0 \sim 10$–20 meV opens, and states near the bottom of conduction band become heavy. This initial reduction of the energy scale is characterized by the parameter ζ_c [Eq. (30)], and the position of the f level relative to the bottom and top of the bare conduction band ϵ_k can be extracted from the ratio of effective masses

$$r \equiv \frac{\varepsilon_{fb}}{\varepsilon_{ft}} = \left(\frac{\zeta_v}{\zeta_c}\right)^{1/2} \approx \left(\frac{m_c^*}{m_v^*}\right)^{1/2}, \quad (44)$$

where $\varepsilon_{ft} = \varepsilon_{k_t} - \varepsilon_f$, ϵ_{k_t} is the top of the band ϵ_k, and the parameter $\zeta_v = (V_0/\varepsilon_{ft})^2$ is determined similarly to ζ_c. We neglect in these crude estimates the anisotropy of hybridization integral $V(\mathbf{k})$. The hole effective mass m_v^* is evaluated as $\sim(500$–$1000) m_0$,[2,5] so we take $r \sim 1/3$, which is consistent with our assumption that the mean-field hybridization gives only part of the actual value of the valence n_v. According to our previous calculations,[22] the value of $r = 1/3$ corresponds to $\overline{n_f} \approx 0.75$, and the experimentally observed value of $n_v \approx 2.55$ can be reached *only* by means of excitonic mechanism, with the exciton mixing parameter $\sin\theta \sim 0.55$ [see Eq. (26)]. This value, in turn, agrees with our assumption of a soft excitonic mode. Then, from Eq. (10), $\zeta_c = 0.01$, and taking for the bandwidth $\varepsilon_{fb} + \varepsilon_{ft}$ the value of 4 eV in accordance with the band calculations for the related system,[18] we estimate the hybridization coupling constant as $V_0 \approx 0.1$ eV which is a reasonable value for the rare-earth materials. To make these estimates self-consistent, a hybridization gap should be found. The gap is defined via the above parameters as $\Delta_0 \approx \zeta_c \varepsilon_{fb} + \zeta_v \varepsilon_{ft}$. Inserting the values of corresponding parameters, we find $\Delta_0 \approx 13$ meV which is in a reasonable agreement with the experimental data.

Now, turning to n-doped materials, we deal with heavy electrons, which interact with the valence fluctuations. The kinetic energy of these electrons is estimated as $\sim V_0^2/\varepsilon_{fb} \sim 10^{-2}$ eV, and the energy scale of valence fluctuations is, by their origin, limited from above by an energy gap of the same 10^{-2} eV width. The polarization coupling constant W_{vf} [Eq. (32)], as well as the ''superhybridization'' matrix elements W in the Hamiltonian (22), should be at least an order of magnitude less than the mean-field hybridization V, so the value of $w_0 = 25$ meV, which is used in our numerical solution of Fig. 3, looks realistic. Eventually, solving Eq. (43) for the polaron shift, we descend one more step along the energy scale and find ourselves in a meV region. The propagation of a self-trapped electron-polaron can in principle be characterized by even lesser energies of the order of 10^{-1} meV.

Thus we have found that heavy electrons near the bottom of the conduction band can propagate in a lattice only in a polarization cloud of valence fluctuations. It is worth mentioning that this conclusion correlates partly with a recent proposition of Kasuya,[29] in spite of the fact that his model of

the ground state of a mixed-valence semiconductor disagreed with our picture in several respects. He chose the trial wave function for a local singlet (which he calls Kondo singlet) of the form

$$|\tilde{0}_{\mathbf{m}}\rangle = \alpha_{f\mathbf{m}}|0_{\mathbf{m}}\rangle + \alpha_{d\mathbf{m}}A^{\dagger}_{d\mathbf{m}}|\psi_{\mathbf{m}}\rangle \tag{45}$$

where $A^{\dagger}_{d\mathbf{m}} = d^{\dagger}_{\mathbf{m}}c_{d\mathbf{m}}$ is a charge-transfer operator, which creates an electron in a $5d$ shell of Sm ion and a hole of d symmetry spread over surrounding boron sites similarly to our f-like orbital $P_{\mathbf{m}}$ entering the state $|\psi_{\mathbf{m}}\rangle$ [Eq. (21)]. The physical reason for such a choice is the conviction that the $5d$ electrons also constitute a strongly correlated subsystem and have a tendency to form a bonding Kondo-like state *à la f* states in conventional Kondo lattices. However, looking at the real band structure of the rare-earth hexaborides, we see that the admixture of d states to the band ϵ_k is very small: the center of gravity of d states in divalent hexaborides is at an energy of $\sim 7-8$ eV above the bottom ϵ_{k_b} of the conduction band (see, e.g., Fig. 5 in Ref. 17). Therefore, $5d$ levels are practically unoccupied, and one cannot expect any kind of effective screening in a d channel. Nevertheless, our model includes an effective screening of *excess* electrons in the conduction band which resembles Kasuya's mechanism: the canonically transformed operators $\tilde{c}_{\mathbf{0}}$ in the weak-coupling limit can be presented as $\tilde{c}_{\mathbf{0}} \sim c_{\mathbf{0}}(1+\alpha A^{\dagger}_{\mathbf{0}})$, and the operator $A^{\dagger}_{\mathbf{0}}$ returns part of the charge density back to the Sm site from the periphery of the unit cell, i.e., plays the same role as the operator $A^{\dagger}_{d\mathbf{0}}$ in trial function (45). The screening (or polaron dressing) in our model is due to the same valence fluctuations as all other physical effects, so the totality of the experimental data is explained in a self-consistent scheme without appealing to any additional hypotheses. As a result, our model is free from undesirable features of the ''Kondo insulator'' approach which are not confirmed by the experiment.

(i) We do not appeal to the Kondo mechanism of forming the ground-state singlet, and the independence of the activation gap on external magnetic field,[30] which rules out the Kondo insulator mechanism, agrees well with the expectations of our model.

(ii) The ground state of our Hamiltonian is absolutely homogeneous, and this statement agrees fairly well with available experimental observations, whereas the trial function (45) implies charge modulation in a form of Wigner crystal or Wigner liquid.[29]

(iii) The model of Ref. 29 gives a single gap which predetermines electronic, optical, and magnetic properties of the material, and it is unclear whether it is compatible with a real experimental situation which definitely evidences several energy scales for electronic and optical characteristics of SmB_6.[5,8]

(iv) Unlike the bare ground state $|0\rangle$, the wave function (45) is not fully symmetrical, so one can expect a sort of ferroelectric ordering as $T \to 0$.[31,32]

Turning to the problem of low-temperature transport, we conclude that as $T \to 0$ the electron propagation is valence-fluctuation-assisted motion of an extremely narrow ''polaron band'' separated by a gap Δ_{act} from the conduction-band continuum. The residual resistivity ρ_0 is inversely proportional to the hopping rate between two neighboring crystal cells,

$$\rho_0^{-1} \sim S_{\mathbf{mn}} \sim T_{\mathbf{mn}}\Phi_{\mathbf{mn}}, \tag{46}$$

where $\Phi_{\mathbf{mn}} = \langle \overline{\psi}_{\mathbf{m}}|\overline{\psi}_{\mathbf{n}}\rangle$ is a function describing the overlap of the valence fluctuation ''clouds'' centered around the sites **m** and **n**. As $T \to 0$ the process is elastic, so the conductivity is temperature independent. In SmB_6 this type of conductivity is observed for $T < 3$ K.[3,5,8] At higher T the hopping is, apparently, assisted by phonon and exciton emission or absorption. Of course, the temperature dependence of this hopping can differ from that for usual variable range hopping in impurity bands. This transient regime can be seen in the range $3\ \mathrm{K} < T < 6$ K, although the experimental data on the temperature dependence are still ambiguous.[3,5,8] In the temperature interval $6\ \mathrm{K} < T < 14$ K, thermally activated resistivity in SmB_6 with an activation energy of $\Delta_{act} \approx 3.5$ meV is observed.[2–5,8] At higher temperatures the electrons dissociate from their local valence fluctuation clouds, and, as a result of this detrapping, find themselves at the bottom of the conduction band. At these temperatures the activation of valence electrons also gives a significant contribution to the electron conductivity.

The same three regimes (III, II and I, respectively, in terms of Ref. 5) with an additional pronounced maximum around 5 K, are observed in the temperature behavior of the Hall constant $R_H(T)$.[4] This maximum can be explained, at least qualitatively, within a simple phenomenological picture of two groups of carriers with high and low electron mobilities, $\mu_b = cR_b\sigma_b$ and $\mu_h = cR_h\sigma_h$, where $R_{b,h}$ and $\sigma_{b,h}$ are the Hall constants and conductivities of light (b) and heavy (h) carriers, respectively. In the case of hopping in impurity bands of doped semiconductors,[33] two contributions σ_h (hopping) and σ_b (band) in the electron conductivity result in the following equation for the Hall constant:

$$R_H = \frac{R_b\sigma_b^2 + R_h\sigma_h^2}{(\sigma_b+\sigma_h)^2}. \tag{47}$$

Then the maximum in $R_H(T)$ corresponds to a crossover from hopping motion at low T to band motion at high T, provided $\mu_b \gg \mu_h$. In our case the phenomenological background of this equation still exists, but the microscopic origin of all temperature dependences should be revised because of the essentially many-particle nature of heavy carriers.

First of all, it is clear that the standard estimates of the number of ''scattering centers'' obtained from the value of the residual resistivity ρ_0 are simply inapplicable in our case, since we deal with hopping of many-particle electron-exciton complexes rather than with the motion of extended band electrons. Thus, there is no room for unitarity limit arguments in these estimates, and the ''superunitarity scattering'' reflects the many-particle nature of current carriers in semiconductors with fluctuating valence.[34] Thus the paradox of the number of scatterers per site[4] is removed, and we return to the usual situation with one scatterer per unit cell.

The next question is the enormously strong pressure dependence of the residual resistivity and the Hall coefficient.[4] Again, according to our model, one cannot directly apply the notions of charge transport in a band of extended states for an estimation of the carrier concentration. We think that the key to the extraordinary sensitivity of the residual resistivity ρ_0 and $R_H(T\to 0)$ to external pressure is *the increase of Sm valence with growing pressure P*. The eventual source of this increase is growing fp hybridization. Because of increasing valence n_v as a function of pressure the matrix element W_{vf} [Eq. (32)] decreases. As a result the polaron shift ε_{pol} as well as the binding energy of the self-trapped electron also decrease. The excitonic overlap function $\Phi_{\mathbf{mn}}$ also grows due to lattice contraction. Since both the hopping integral $T_{\mathbf{mn}}$ and the function $\Phi_{\mathbf{mn}}$ depend exponentially on the intersite distance, one can expect a very sharp dependence of the hopping rate on external pressure. The radius of the localized state with binding energy 3.5 meV and effective mass $\sim 100 m_0$ is estimated to be 2–4 Å,[5] and an increase of this radius by an order of magnitude would be enough to obtain a 10^4 growth of the hopping rate. Such an increase is achievable under a pressure of 50 kbar. At higher pressures the trap becomes too shallow (the valence too close to 3) to catch the electron; the system transforms into a conventional *n*-doped degenerate semiconductor, and eventually it becomes a metal with trivalent Sm ions in the cation sublattice.

Finally, the question of the variation of electron concentration n_e with increasing P and T also demands special consideration. Usually information about n_e is extracted from the value of R_H under the assumption of single-band conductivity when $R_H \approx R_b = (n_e e c)^{-1}$. According to the experimental data cited above, R_H is nearly constant in the temperature interval I (below 3 K), but falls drastically with applied pressure: $R_H(45\ \text{kbar})/R_H(1\ \text{bar}) \sim 10^{-4}$. However, in our case of two-component systems with $\sigma_h \gg \sigma_b$ the Hall constant takes the form

$$R_H \approx \frac{\mu_b \sigma_b + \mu_h \sigma_h}{c \sigma_h^2}.$$

It is seen immediately that the pressure dependence of this function is determined mainly by the denominator, and the decrease of R_H with pressure is due to the exponentially growing factor $S_{\mathbf{mn}}$ in Eq. (46) for σ_h rather than to increasing n_e.

Generally speaking, R_H derived from Eq. (47) also cannot be used to determine electron concentration neither in region I nor in region II. The low-T limit of $n_{e0} \sim 10^{17}\ \text{cm}^{-3}$, which is obtained under the assumption that $R_H \approx R_b$, can only be considered as a lower bound. In the general case of two mechanisms of charge transport the Hall constant is $R_H = (n_e e c)^{-1} \mu_H / \mu_D$, where $\mu_{H,D}$ are the Hall and drift mobilities respectively. If $\mu_H / \mu_D \gg 1$ at low T the real electron concentration n_e may substantially exceed the value of n_{e0}. Referring to the exponential dependence of $\sigma(T)$ and $R_H(T)$ in region II, we should note that there are at least two causes of such a dependence. First there is the thermal activation of electrons from the polaronic traps to the band continuum states, and second is the temperature dependence of the hopping rate $S_{\mathbf{mn}}$ due to the contribution of thermally activated exciton-assisted terms which appear instead of the overlap integral $\Phi_{\mathbf{mn}}$. As a result, both $\sigma_h(T)$ and $\sigma_b(T)$ give exponential contributions with an activation energy of $\Delta_{act} \sim 3.5$ meV to the electron conductivity and the Hall constant [Eq. (46)]. Again, it is impossible to calculate the variation of the electron concentration $n_e(T)$ directly from this equation. We leave the detailed evaluation of various transport coefficients for a forthcoming paper, but to conclude this qualitative discussion we would like to emphasize that according to the theory proposed in this paper the total carrier concentration in conduction band is $n_e \sim 10^{17}\ \text{cm}^{-3}$, at least while the interband electron activation is negligible ($T \ll \Delta_0$), and there is no room for dramatic pressure or temperature variation of n_e in the mixed-valence phase of *n*-SmB_6. The real semiconductor to metal transition occurs only at $P > P_c$ when the Sm valence changes to the integer value of $+3$.

In conclusion, we have demonstrated in this paper that the intermediate-valence state is formed in SmB_6 as the result of both conventional mean-field pf hybridization in the electron bands and the excitonic instability which is manifested by the admixture of low-lying singlet charge-transfer excitons to the mean-field ground state. The latter mechanism gives the main contribution to the value of intermediate valence n_v. This instability is a common feature of SmB_6 and SmS, and this is the reason why the value of n_v is practically the same in these two compounds in spite of completely different band spectra.

It is shown also that the motion of strongly hybridized electrons near the bottom of the conduction band is strongly influenced by valence fluctuations. The polarization of intermediate-valent Sm ions induced by these heavy carriers results in a self-trapping similar to electron self-trapping in polar dielectrics, and valence fluctuations play the same role (and have nearly the same characteristic times) as optical phonons in the conventional polaronic effect. Like the small polaron case, self-trapping does not mean a spontaneous breaking of global translation invariance: the electron can be trapped in any crystalline cell, and the mechanism of its propagation at ultralow temperature is exciton-assisted hopping similar to phonon-assisted hopping in a narrow polaron band.

ACKNOWLEDGMENTS

The authors are grateful to M. Aronson, D. I. Khomskii, and N. E. Sluchanko for useful discussions. This work was supported by Israeli Academy of Sciences and Humanities Center for ''Strongly Correlated Interacting Electrons in Restricted Geometries.'' S.C. acknowledges the support of the Feinberg School of the Weizmann Institute.

APPENDIX

Below we describe the self-trapped state of the electron captured by the nonlocal potential (32). For the sake of simplicity we consider the case of conduction band with a minimum at the Γ point of the Brillouin zone. To solve the Dyson equation (36), we offer the procedure of factorization of the vertex matrix element $W_{vf}(\mathbf{k}_1, \mathbf{k}_2)$. The latter can be represented in a form $W_{vf}(\mathbf{k}_1, \mathbf{k}_2) \equiv \Sigma_{a=0}^{8} \gamma_{\mathbf{k}_1}^a \gamma_{\mathbf{k}_2}^a$, where

$$\gamma_{\mathbf{k}}=\begin{pmatrix} \sqrt{w_0} \\ \sqrt{8\zeta w_1}\cos\frac{k_x}{2}\cos\frac{k_y}{2}\cos\frac{k_z}{2} \\ \sqrt{8\zeta w_1}\sin\frac{k_x}{2}\cos\frac{k_y}{2}\cos\frac{k_z}{2} \\ \sqrt{8\zeta w_1}\cos\frac{k_x}{2}\sin\frac{k_y}{2}\cos\frac{k_z}{2} \\ \sqrt{8\zeta w_1}\cos\frac{k_x}{2}\cos\frac{k_y}{2}\sin\frac{k_z}{2} \\ \sqrt{8\zeta w_1}\sin\frac{k_x}{2}\sin\frac{k_y}{2}\cos\frac{k_z}{2} \\ \sqrt{8\zeta w_1}\cos\frac{k_x}{2}\sin\frac{k_y}{2}\sin\frac{k_z}{2} \\ \sqrt{8\zeta w_1}\sin\frac{k_x}{2}\cos\frac{k_y}{2}\sin\frac{k_z}{2} \\ \sqrt{8\zeta w_1}\sin\frac{k_x}{2}\sin\frac{k_y}{2}\sin\frac{k_z}{2} \end{pmatrix} \tag{A1}$$

By writing $G^a_{\mathbf{k}}\equiv\Sigma_{\mathbf{k}'}\gamma^a_{\mathbf{k}'}G_{\mathbf{k},\mathbf{k}'}$, we obtain a solution for G of the form

$$G^a_{\mathbf{k}}(\omega)=(M^{-1})^{ab}\gamma^b_{\mathbf{k}}G^0_{\mathbf{k}}(\omega), \tag{A2}$$

where

$$M^{ab}=\delta^{ab}-\sum_{\mathbf{k}_1\mathbf{k}_2}\sum_{c=0}^{8}G^0_{\mathbf{k}_1}(\omega)\mathcal{P}_{\mathbf{k}_2}(\omega,\Omega_0)\gamma^a_{\mathbf{k}_1}\gamma^c_{\mathbf{k}_1}\gamma^c_{\mathbf{k}_2}\gamma^b_{\mathbf{k}_2}. \tag{A3}$$

Here the index $a=0$ corresponds to the fully symmetric solution described approximately by Eq. (39), and $a=1$ stands for the nonlocal contribution of the ''tail'' w_1 with the same A_1 symmetry. For the indices $a,b=2,\ldots,8$ the matrix M is actually diagonal since terms in the integrand must be even in k_{1x},k_{1y},k_{1z}, and k_{2x},k_{2y},k_{2z} and therefore $a=c=b$. For these components M is given by

$$M^{ab}=\delta_{ab}[1-m^a(\omega)m^a(\omega-\Omega_0)],\quad a,b=2,\ldots,8. \tag{A4}$$

For the components $a,b=0,1$ M reduces to a 2×2 matrix

$$M=\begin{pmatrix} 1-m^1(\omega)m^0(\omega-\Omega_0) & -m^0(\omega)\tilde{m}(\omega-\Omega_0) \\ -\tilde{m}(\omega)\tilde{m}(\omega-\Omega_0) & -\tilde{m}(\omega)m^1(\omega-\Omega_0) \\ -\tilde{m}(\omega)m^0(\omega-\Omega_0) & 1-\tilde{m}(\omega)\tilde{m}(\omega-\Omega_0) \\ -m^1(\omega)\tilde{m}(\omega-\Omega_0) & -m^1(\omega)m^1(\omega-\Omega_0) \end{pmatrix}. \tag{A5}$$

In Eqs. (A4) and (A5), $m(\omega)$ is given by

$$m^a(\omega)=\sum_{\mathbf{k}}G^0_{\mathbf{k}}(\omega)(\gamma^a_{\mathbf{k}})^2,\quad a=0,\ldots,8, \tag{A6}$$

$$\tilde{m}(\omega)=\sum_{\mathbf{k}}G^0_{\mathbf{k}}(\omega)\gamma^0_{\mathbf{k}}\gamma^1_{\mathbf{k}}. \tag{A7}$$

Thus we find that M is reducible to the different representations of the group of symmetry operations on an octahedron O_h: $a=0$ and 1 and $a=8$ stand for the one-dimensional representations A_1 and A_2, respectively, while $a=2$, 3, and 4, and $a=5$, 6, and 7 are the indices of triplet states T_1 and T_2.

Hence, the secular equation which generalizes Eq. (39) has the form (for $\zeta\ll1$):

$$0=\mathrm{Det}\,M=[1-m^0(\omega)m^0(\omega-\Omega_0)-2m^1(\omega)m^1(\omega-\Omega_0)]\prod_{a=2}^{8}[1-m^a(\omega)m^a(\omega-\Omega_0)], \tag{A8}$$

$$m^{A_1,T_1,T_2,A_2}(\omega)=w_1\int_{-\pi}^{\pi}\frac{dk_xdk_ydk_z}{(2\pi)^3}\frac{\zeta(1\pm\cos k_x)(1\pm\cos k_y)(1\pm\cos k_z)}{\omega-\epsilon(\mathbf{k})}. \tag{A9}$$

Here the choice of three + signs corresponds to the A_1 state, two + signs corresponds to the T_1 triplet, two − signs corresponds to the T_2 triplet, and three − signs corresponds to the singlet A_2. To study the analytical properties for small $\omega<0$, we use the fact that the dominant contribution to the integral comes from small values of $\mathbf{k}$. Near the bottom of conduction band $\varepsilon_2(\mathbf{k})$ the hybridization is strong, and the band is nearly flat [see Eq. (4)], so expanding the dispersion around the minimum at the bottom, $\varepsilon(k)\approx\hbar^2k^2/2m^*$ in accordance with Eq. (9), we refer to the heavy effective mass of $m^*\approx100m_0$, observed experimentally.[5,8] Then we find for, small $\omega<0$,

$$m^0(\omega)\approx\frac{w_0}{\epsilon_0}\left(-0.39+\frac{1}{2\pi}\sqrt{\frac{2|\omega|}{\epsilon_0}}\right), \tag{A10}$$

$$m^1(\omega)\approx\frac{\zeta w_1}{\epsilon_0}\left(-1.31+\frac{1}{2\pi}\sqrt{\frac{2|\omega|}{\epsilon_0}}\right), \tag{A11}$$

$$m^{T_1}(\omega)\approx\frac{\zeta w_1}{\epsilon_0}\left(-0.35+0.28\frac{|\omega|}{\epsilon_0}\right), \tag{A12}$$

$$m^{T_2}(\omega) \approx \frac{\zeta w_1}{\epsilon_0}\left(-0.20+0.05\frac{|\omega|}{\epsilon_0}\right), \tag{A13}$$

$$m^{A_2}(\omega) \approx \frac{\zeta w_1}{\epsilon_0}\left(-0.14+0.02\frac{|\omega|}{\epsilon_0}\right), \tag{A14}$$

where $\epsilon_0=\hbar^2/a^2m^*\approx 5$ meV. Solutions of Eq. (A8) for the values of the parameters given in Fig. 3 yield no bound states for T_1, T_2, and A_2, so we conclude that the approximation $W_{vf}\approx w_0$ for potential (32) is sufficient for the description of the bound electron-exciton states.

*Electronic address: kikoin@bgumail.bgu.ac.il

[1] E.E. Vainstein, S.M. Blokhin, and Yu.B. Paderno, Sov. Phys. Solid State **6**, 281 (1965).

[2] P. Wachter, in *Handbook on the Physics and Chemistry of Rare Earths*, edited by by K.A. Gschneider, Jr. and L. Eyring (North-Holland, Amsterdam, 1994), Vol. 19, p. 177.

[3] I. Bat'ko, P. Farkašovský, K. Flachbart, E.S. Konovalova, and Yu.B. Paderno, Solid State Commun. **88**, 405 (1993); S. Gabáni, K. Flachbart, P. Farkašovský, V. Pavlík, I. Bat'ko, T. Herrmannsdörfer, E. Konovalova, and Y. Paderno, Physica B **259-261**, 345 (1999).

[4] J.C. Cooley, M.C. Aronson, Z. Fisk, and P.C. Canfield, Phys. Rev. Lett. **74**, 1629 (1995).

[5] N.E. Sluchanko, A.A. Volkov, V.V. Glushkov, B.P. Gorshunov, S.V. Demishev, M.V. Kondrin, A.A. Pronin, N.A. Samarin, Y. Bruynseraede, V.V. Moshchalkov, and S. Kunii, JETP **88**, 533 (1999).

[6] G. Travaglini and P. Wachter, Phys. Rev. B **29**, 893 (1984).

[7] H. Ohta, R. Tanaka, M. Motokawa, S. Kunii, and T. Kasuya, J. Phys. Soc. Jpn. **60**, 1361 (1991); T. Nanba, H. Ohta, M. Motokawa, S. Kimura, S. Kunii, and T. Kasuya, Physica B **186-188**, 440 (1993).

[8] M. Dressel, B. Gorshunov, N. Sluchanko, A. Volkov, G. Knebel, A. Loidl, and S. Kunii, Physica B **259-261**, 377 (1999); B. Gorshunov, N. Sluchanko, A. Volkov, M. Dressel, G. Knebel, A. Loidl, and S. Kunii, Phys. Rev. B **59**, 1808 (1999).

[9] G. Güntherodt, W.A. Thompson, F. Holtzberg, and Z. Fisk, Phys. Rev. Lett. **49**, 1030 (1982).

[10] K.A. Kikoin, Zh. Éksp. Teor. Fiz. **85**, 1000 (1983) [JETP **58**, 582 (1983); J. Phys. C **17**, 6771 (1984).

[11] P.A. Alekseev, A.S. Ivanov, B. Dorner, H. Schober, K.A. Kikoin, A.S. Mishchenko, V.N. Lazukov, E.S. Konovalova, Yu.B. Paderno, A.Yu. Rumyantsev, and I.P. Sadikov, Europhys. Lett. **10**, 457 (1989); K.A. Kikoin and A.S. Mishchenko, J. Phys. Condens. Mater. **3**, 5937 (1991); K.A. Kikoin and A.S. Mishchenko, Zh. Éksp. Teor. Fiz. **77**, 828 (1993) [JETP **104**, 3810 (1993)].

[12] J. Neuenschwander and P. Wachter, Phys. Rev. B **41**, 12 693 (1990).

[13] D.P. Young, D. Hall, M.E. Torelli, Z. Fisk, J.L. Sarrao, J.D. Thompson, H.-R. Ott, S.B. Oseroff, R.G. Goodrich, and R. Zysler, Nature (London) **397**, 412 (1999).

[14] M.E. Zhitomirsky, T.M. Rice, and V.I. Anisimov, cond-mat/9904330 (unpublished); L. Balents and C.M. Varma, cond-mat/9906259 (unpublished); V. Barzykin and L.P. Gor'kov, cond-mat/9906401 (unpublished).

[15] F.C. Zhang and T.M. Rice, Phys. Rev. B **37**, 3759 (1988).

[16] A. Hasegawa and A. Yanase, J. Phys. C **12**, 5431 (1979).

[17] S. Massida, A. Continenza, T.M. de Pascale, and R. Monnier, Z. Phys. B: Condens. Mater. **102**, 83 (1997).

[18] H. Harima, O. Sakai, T. Kasuya, and A. Yanase, Solid State Commun. **66**, 603 (1988).

[19] A. Yanase and H. Harima, Prog. Theor. Phys. Suppl. **108**, 19 (1992).

[20] R.M. Martin and J.W. Allen, J. Appl. Phys. **50**, 7561 (1979).

[21] S.E. Barnes, J. Phys. F: Met. Phys. **6**, 1375 (1976).

[22] K.A. Kikoin, Solid State Commun. **33**, 323 (1980).

[23] K.W.H. Stevens, J. Phys. C **11**, 985 (1978).

[24] V.J. Emery, Phys. Rev. Lett. **58**, 2794 (1987).

[25] V.I. Belinicher and A.L. Chernyshev, Phys. Rev. B **49**, 9746 (1994).

[26] J.C. Nickerson, R.M. White, K.N. Lee, R. Bachman, T.H. Geballe, and G.W. Hull, Phys. Rev. B **3**, 2030 (1971).

[27] Y. Toyozawa, in *Relaxation of Elementary Excitations*, edited by R. Kubo and E. Hanamura (Springer, Berlin, 1980), p. 3.

[28] I.G. Lang and Yu.A. Firsov, Zh. Éksp. Teor. Fiz. **43**, 1843 (1962) [Sov. Phys. JETP **16**, 1301 (1963)].

[29] T. Kasuya, Europhys. Lett. **26**, 277 (1994).

[30] J.C. Cooley, M.C. Aronson, A. Lacerda, Z. Fisk, P.C. Canfield, and R.P. Guertin, Phys. Rev. B **52**, 7322 (1995).

[31] T. Portengen, Th. Östreich, and L.J. Sham, Phys. Rev. B **54**, 17 452 (1996).

[32] See K.A. Kikoin and A.S. Mishchenko, J. Phys.: Condens. Matter **7**, 307 (1995) for more comments on the approach based on *d*-electron screening.

[33] B.I. Shklovskii and A.L. Efros, *Electronic Properties of Doped Semiconductors* (Springer, Berlin, 1984).

[34] C. Varma, in *Windsurfing the Fermi Sea*, edited by T.T.S. Kuo and J. Speth (North-Holland, Amsterdam, 1987), p. 69.